BIU Journal of Basic and Applied Sciences 9(2): 186 – 197, 2024.

ISSN: 2563-6424

BORATES-STABILIZED SILVER NANOCLUSTERS: POST-SYNTHESIS LIGANDS EXCHANGE REACTION WITH CYSTEINE

***OYEM, H. H [1, 2] AND OYEM, I. M.[3]**

[1]School of Chemistry, Newcastle University, Newcastle Upon Tyne, United Kingdom
[2]Department of Chemical Sciences, Faculty of Science, University of Delta, Agbor, Delta State
[3]Department of Biological Sciences, Faculty of Science, University of Delta, Agbor, Delta State
*Corresponding author: hector.oyem@unidel.edu.ng

ABSTRACT

The lability of the inorganic capping ligands on silver nanoclusters (Ag NCs) formed by the microemulsion method was studied in an exchange reaction with cysteine amino acid in aqueous conditions. The essence was to study the feasibility of this exchange reaction in vivo systems with similar biomolecules especially in the field of medicine and drug delivery systems mimicking antigens–antibody reactions in immunology and immunochemistry. Ag NCs were synthesized in microemulsion droplets. Transmission electron microscope (TEM) shows the formation of these Ag nanocrystals on a holey carbon grid. The crystals were approximately 2 nm in average size, generally spherical and monodispersed. Fourier transform infrared spectroscopy (FT-IR) was used to monitor the reaction by observing the disappearance and significant changes in the vibrational frequencies between the inorganic ligand-stabilized Ag NCs which served as the control, and the new Ag(cysteine) complex. The FT-IR result confirmed the formation of the Ag(cysteine) molecule with the binding site seemingly on the nitrogen atom of the amine group of the cysteine molecule. The resulting new compound was considered to be a zwitterion with a carboxylate ion end group which is prone to switching into a resonance hybrid structure with the delocalization of the electron charge of the carboxylate group. Electrospray ionization mass spectrometer (ESI-MS) data confirmed the molecular mass and formula of the new Ag(cysteine) complex and the successful ligand exchange reaction.

KEYWORDS: *Ligand, Exchange reaction, Microemulsion, Ag NCs, Cysteine, Vibrational frequency*

INTRODUCTION

Nanoparticles (NPs) refer to nanoscale materials in the dimension range of 1 to 100 nm (Selmani *et al*., 2022). This is the generic term that describes all nanometer-sized materials but is usually adopted for bigger nanomaterials than for the smaller nanoclusters (NCs) of less than 2 nm sizes. Metal nanoparticles are therefore nanomaterials made from metal ion precursors with nanosize dimensions. Among these are notably, Ag, Au, and Cu which together are referred to as coinage metal nanoparticles (MNPs) (Basu *et al*.,

2024, Liu *et al*., 2024 and Michos *et al*., 2024). Attention is given to these sub-microscopic (that is, electron microscopic) size materials because of the remarkable deviation from the bulk material properties to those of molecule-like physical properties (Selmani *et al*., 2022). They thus exhibit quite impressive physico-optical properties which are unique for metals ordinarily (Joudeh and Linke, 2022).

Scientists have since studied and harnessed these interesting nanoscale-physical properties and applied them to almost all areas of life for unprecedented product enhancements as well as technological advancement. However, these quantum-size materials which attain sizes and morphologies that vary extensively with the methods of synthesis, synthesis conditions, and stabilizing agents are thermodynamically unstable and need to be stabilized (Phan and Haes, 2019). Stabilizing agents are accompanying ligands that accord protective stability to the NPs from spontaneous growth typically referred to as Oswald Ripening (An *et al*., 2022).

Oswald ripening is the self-assembling inevitable growth that accompanies NPs after the nucleation stage of synthesis. This is in response to the thermodynamic need to reduce their large surface-to-volume ratio (Bawoke and Abera, 2023, Joudeh and Linke, 2022). Stabilizers in nanoscience and nanotechnology are replete, although the majority are remarkably of organic basis. The most notable is DNA – both oligos and duplexes. These molecules are usually coordinated to the metal conjugate by coordinate bonding (covalency).

One of the focus of the nanomaterial research and growth is in the field of food and medicine (Lan, 2022, Nile *et al*., 2020, Shafiq *et al*., 2020, Soares *et al*., 2018). These find expression in sensing (detection) and drug delivery systems (Bardhan, 2022, Jadhav *et al*., 2024, and Jebasingh *et al*., 2023). The crucial points lie in the ability to specifically and successfully bind nanoprobes to target biomarkers and being able to record the subsequent changes in the physicochemical properties of the new conjugate.

In the areas of drug delivery, antigen and antibody reactions (immunology and immunochemistry), nanoscientists and nanotechnologists have evolved mimicking models to serve as probes for specific targets (Ashique *et al*., 2023, Fernández-gómez *et al*., 2023, and Poon *et al*., 2020). However, for these to be effective there must be the possibility to establish successful and effective stable bonding with the target biomolecule. Such connections are only likely if the ligands attached to the NPs are labile. Lability is the ease by which a ligand can be exchanged by another.

NPs are preferably prepared by first, attaching the metal ion to the stabilizing ligand before reduction with an appropriate reducing agent. However, in *in vivo* situations, NPs are already formed *in vitro* before introduction to the body, hence only conjugation with the target biomolecules including on cell membranes, and subsequent endocytosis can be anticipated. In this present study, the possibility of exchanging the borate (and borane) ligand on Ag NCs post-synthesis and replacing them with cysteine is simulated *in vitro*.

MATERIALS AND METHODS

Material

Silver nitrate ($AgNO_3$, 99.0%, 25 g), sodium borohydride ($NaBH_4$, 99.0%, 25 g), and L-cysteine amino acid ($HSCH_2CH(NH_2)COOH$, 97.0%) were purchased from Sigma Aldrich, USA. Sodium bis-(2-ethyl hexyl) sulfosucinate (commercial name, Docusate sodium or simply as AOT) ($C_{20}H_{37}NaO_7S$) was also bought from Sigma Aldrich, U.S.A as well as 2, 2, 4-trimethylpentane (isooctane, 99.8%). Deionized water was obtained from Millipore Diamond Barnstead series 1370, a model manufactured by Barnstead International, Iowa, USA.

Methods

Synthesis of Silver Nanoclusters in Microemulsion System

Silver nanoclusters Ag NCs (0.09 mM) were synthesized in microemulsion droplets using AOT as a surfactant according to the synthesis protocol by Oyem (2018). A 500 μL portion of the sample was pipetted into a separating funnel mounted on a retort stand and 500 μL deionized water was added to achieve phase separation of the organic and aqueous portions. This was allowed to stand for 5 minutes before the aqueous phase was collected into a clean glass vial. The solution was subsequently passed through a Restec cartridge containing a reverse phase gel to further remove traces of organic solvent and AOT using the vacuum pump system in a fumehood before further analysis and reaction with cysteine.

Reaction of Silver Nanoclusters with L-Cysteine (Ligand exchange)

A stock solution of aqueous L-cysteine was prepared from which 0.015 mM was subsequently obtained in a final volume of 100 μL. This was added to the eluted as-synthesized sample portion in the Eppendorf tube and vortexed for 3 minutes, and then allowing it to stand overnight before analysis.

Characterization Techniques

Preparation of samples for Transmission Electron Microscopy (TEM) Analysis

2 μL portions of the as-synthesized Ag NCs were drop-cast onto to clean holey carbon grid and allowed to air-dry covered in clean aluminum foil under vacuum overnight before TEM analysis on a Phillips CM 100 instrument. The instrument works by sending a strong beam of electrons under high voltage which are reflected by the samples from which microscopic images are obtained.

Preparation of Samples for Electrospray Ionization Mass Spectroscopy (ESI-MS) Analysis

10 μL of the cartridge eluted sample was withdrawn into small Eppendorf tubes and further diluted with 1000 μL of deionized water in a ratio of 1: 100. The sample was run in both the positive and negative mode of the instrument. A control analysis consisting only of the eluted sample without the cysteine was similarly run on the ESI-MS machine a product of Waters LCT Premier time-of-flight Electrospray ionization mass spectrometer, USA.

Preparation of Samples for Fourier Transform Infrared (FT-IR) Analysis

1 μL portions of the sample was withdrawn using a micropipette onto the sample port of the instrument which has been thoroughly cleaned with acetone and baseline calibrated before obtaining the IR spectrum of the sample from an IR Affinity, Shimadzu instrument, made in Japan. A control spectrum of only a solution of the cysteine was also obtained from the instrument. Several runs were taken to obtain an optimized spectrum of

the samples bearing in mind that they are highly dilute sample solutions.

RESULT AND DISCUSSION

The results of the TEM, FT-IR, and ESI-MS of the samples are shown in Figures 1, 2 and 3 below.

Transmission electron microscopy (TEM)

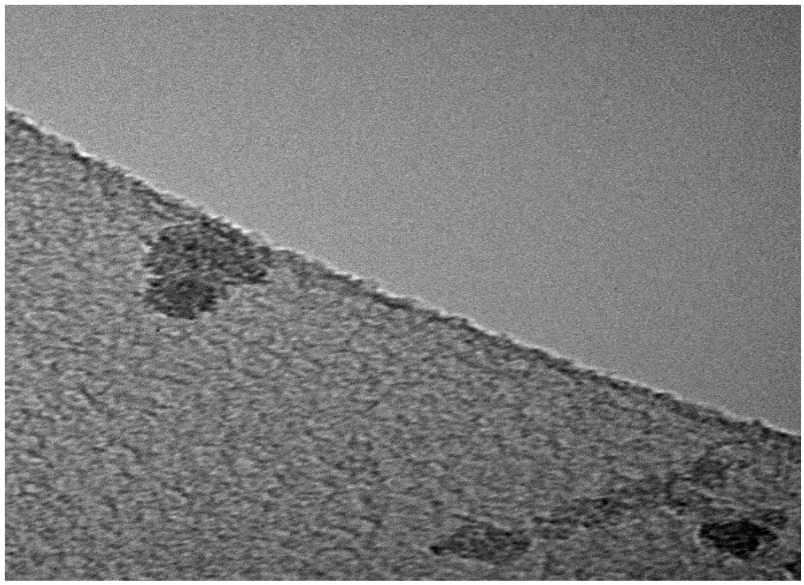

Fig. 1: TEM images of the Ag NCs on a holey carbon grid showing tiny black, spherical crystals of Ag NCs before the reaction with cysteine

Figure 1 is a TEM image showing that Ag NCs have been synthesized by the microemulsion system; these NCs are seemingly spherical nano-sized particles. The scale on the sample images can provide a quick indication of how small these Ag NCs are in terms of their sizes (Oyem *et al*., 2022). However, the actual particle size can only be confirmed by a particle size analyzer, but in the absence of data from the particle size analyzer, one can deduce from these images that these Ag NCs are around 2 nm size particles or less which technically qualifies them as Ag NCs. The images show dark, spherical crystals of Ag NCs surrounded by surfactant matrix. Nonetheless, these TEM images in Figure 1 demonstrate that Ag NCs have been synthesized.

Fourier transform infrared (FT-IR)

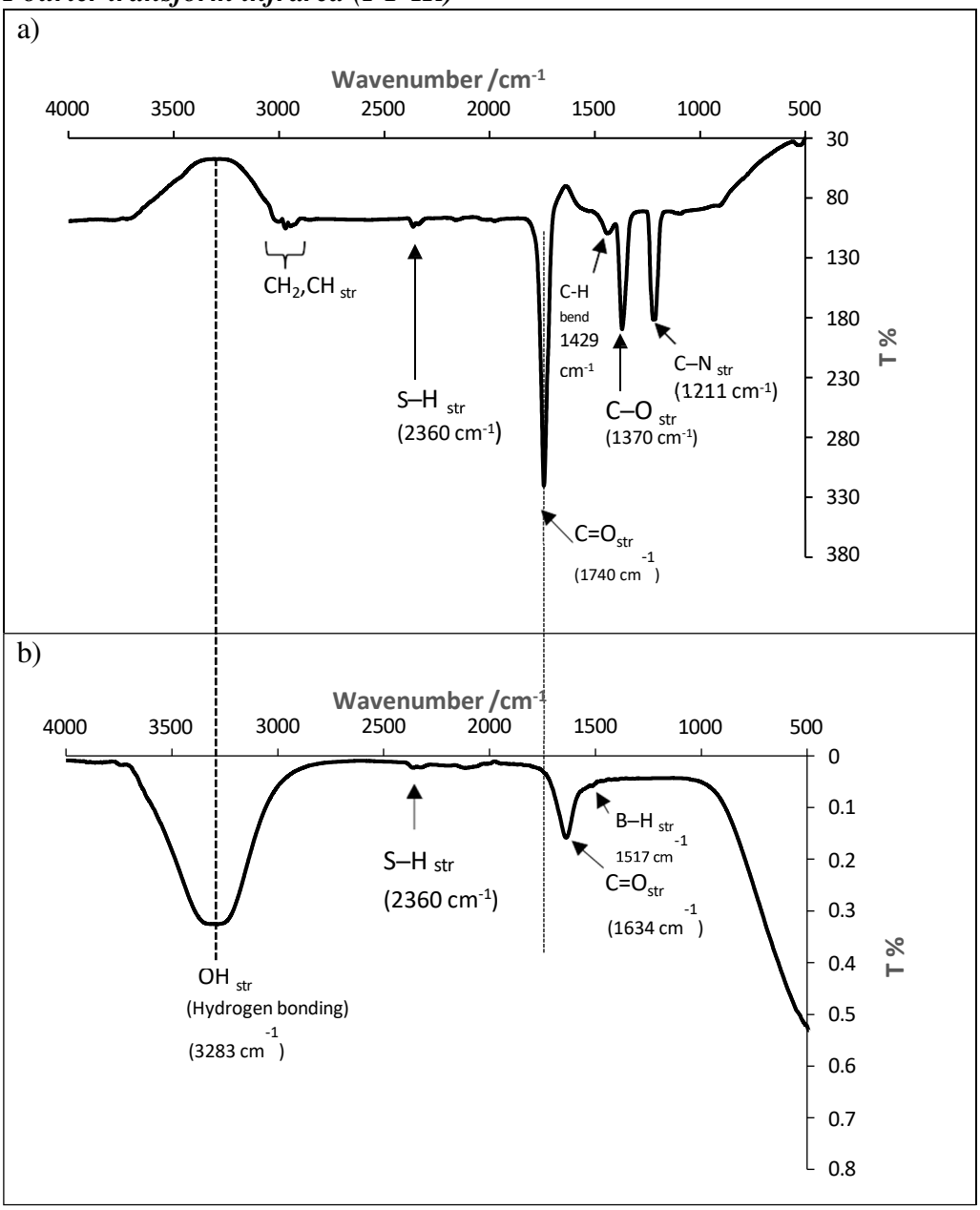

Fig. 2: FT-IR spectrum of **a**) cysteine, **b**) (Ag_n(Cysteine)).

To specifically classify the functional groups of the stabilizing ligands present in the samples' FT- IR spectra of both the borate and cysteine stabilized Ag NCs before and after the ligand exchange reaction with cysteine molecule were obtained. Figures 2a&b are FT-IR spectra of cysteine and cysteine-conjugated Ag NCs respectively. FT-IR technology is a sensitive analytical tool to detect the signature vibrational frequencies in a molecule. The spectrum in Figure 2a shows vibrational bands corresponding to C=O str., CH_2, CH str., the N-H str., and the

OH $_{str}$ of the carbonyl, methyl and methylene, the amine, and hydroxyl groups respectively (Khalkho *et al*., 2020). These can be found at 1740, 2862 - 3032, and 3283 cm^{-1} accordingly in the FT-IR spectrum of the cysteine molecule which served as the control. The latter OH $_{str.}$ band of course is broad and intense as would be expected due to hydrogen bonding (Athokpam *et al*., 2017). While the two bands at 1211 and 1340 cm^{-1} have been assigned to the C─N and C─O $_{str.}$ vibrations (Hasegawa, 2017, and Smith, 2017). However, after the ligand exchange reaction, we can observe the disappearance of some of the bands previously seen in the cysteine spectrum. Typical among these are the C─O and the C─N $_{str.}$ vibrations of the cysteine molecule. Besides these, there were also the disappearance of the CH_2 and CH $_{str.}$ at 2967 cm^{-1} as well as the NH_2 band, (Wang *et al*., 2023) although, it is believed that these bands have been subsumed by the very broad hydrogen bonding at 3283 cm^{-1} in Figure 2b above. The summary of the IR bands from the sample is presented in Table 1 below.

Table 1: Summary of the various vibrational bands in the IR spectra

IR vibrational band	C=O (str)	CH_2, CH (str)	N─H (str)	O─H (str)	C─N (str)	C─O (str)	S─H (str)	B–H (bend)
Frequency (cm^{-1})	1750	2800 - 3000	3300 - 3500	3200 - 3600	1211	1340	2360	1517

C=O Stretching vibration

Perhaps the most remarkable observation from both spectra can be observed in the carbonyl functional group. The original band of the C=O $_{str.}$ vibration was recorded at 1740 cm^{-1} frequency (Khalkho *et al.*, 2020) before the ligand exchange reaction, however, there was a notable change in this famous vibrational band after the exchange reaction. This is considered an obvious demonstration of the establishment of a new bond on the cysteine molecule. It shows that bonding has occurred on the cysteine molecule post-exchange reaction.

Theoretically, the attachment of an electron-donating group to the second oxygen atom on the single-bonded carbon-oxygen of the carboxylic acid group resulted in a decrease in the vibrational frequency of the carbonyl (C=O) bond thereby causing it to be elongated and weakened causing the electron cloud density to shift more towards the carbonyl oxygen atom (Campanella *et al*., 2021). Conversely, the addition of an electron-withdrawing group to the oxygen atom of the C─O^- end of the carboxylic acid group should cause a shortening (strengthening) of the carbonyl C=O bond due to inductive and mesomeric effects and therefore result in a higher vibrational frequency position (Campanella *et al*., 2021). Similarly, any direct addition to the carbonyl oxygen atom will likewise result in the elongation of the C=O bond to a C─O bond and an inevitable disappearance of the C=O $_{str.}$ band entirely from the spectrum.

In this present study, the C=O band did not disappear after the ligand exchange reaction, signifying that the carbonyl group is intact. However, the shift in frequency position by a value of 106 cm^{-1} from 1740 – 1634 cm^{-1} is a significant decrease in frequency. Since hydrogen bonding similarly affects cysteine molecules before and after the exchange reaction, hydrogen bonding is ruled out as the cause of this major shift in vibrational frequency position. Similarly, direct

coordination of the Ag^+ ion to the carbonyl oxygen would have resulted in the total disappearance of the C=O $_{str.}$ band from the spectrum in Figure 2b. This leaves out the effect of resonance hybrid structure arising from electron delocalization of the carboxylate ion. The carboxylate ion is believed to have been formed considering the neutral condition of this reaction. Thus, making it possible for the solvated carboxylic acid proton to rather combine with water molecules and leave the cysteine amino acid deprotonated.

This implies resonance delocalization of the carboxylate electrons between the carbonyl oxygen and the C─O^-. Invariably, resonance delocalization of the electron cloud is more likely to cause both a shift to lower frequency and a drop in the intensity of the C=O $_{str.}$ band. The changes in frequency position and intensity of the C=O $_{str.}$ band after the exchange reaction is therefore a positive inference that the carboxylic acid proton was lost as a consequence of the ligand exchange reaction as can be seen in Figure 2b. This is deprotonation occurred and resulted in a carboxylate ion being formed (see reaction scheme in Figure 3 below) which subsequently became a resonance hybrid canonical structure (not shown). Ostensibly, this situation best explains the attenuation of the intensity of the C=O $_{str.}$ band and the shift to a lower vibrational frequency position in the spectrum (Figure 2b).

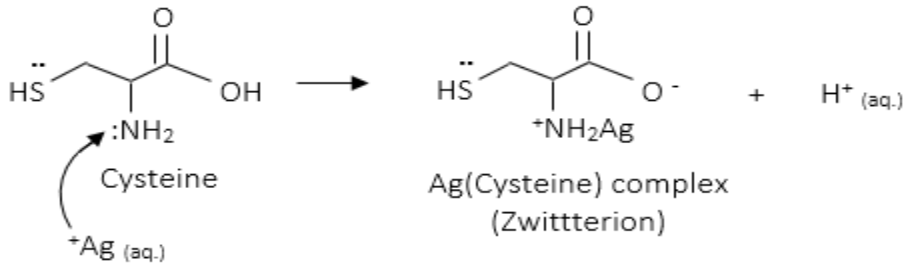

Fig. 3: Reaction scheme for Ag(Cysteine) complex formation

S–H Stretching vibration

It is apparent from Figure 2b that the intensity of the S–H $_{str.}$ weakened after the exchange reaction, which points to the likelihood of the Ag^+ ion coordinating with the mercaptan (-SH) group of the cysteine molecule, hence the loss of intensity of this S–H $_{str.}$ band at 2360 cm^{-1}; even though, the S–H bond remained intact (Khalkho *et al*., 2020).

B–H Stretching/bending vibration

The B–H $_{str}$ of the borohydride (BH_4^-) also appears in the same region around 2400 – 2500 cm^{-1} as the S–H $_{str}$ (Deniz *et al*., 2022; Hagemann *et al*., 2008; Paunkovic *et al*., 2013) with B–H $_{bend}$ vibration occurring around 1531 cm^{-1} (Hageman 2008) which seems to be the poorly resolved weak band appearing at 1517 cm^{-1} in Figure 2b. The weakness of the band is attributed to the extremely low concentration of the sample, although some of these signals have characteristically weak signal intensities.

C─O Stretching/bending vibration

The C─O $_{str.}$ band is thought to have disappeared in the spectrum in Figure 2b because of the formation of the

carboxylate ion. However, as the carboxylate group contains an oxygen anion (C─O^-) that is capable of being delocalized thereby resulting in a resonance hybrid, the single bond character of the C─O bond is no longer stable but more likely to switch between the single and double bond character in the resulting resonance structure. Hence there is no stable C─O $_{str.}$ vibration in the IR spectrum of the new Ag(Cysteine) molecule as was confirmed in Figure 2b.

C─N Stretching vibration

It is believed that the C─N $_{str.}$ also disappeared in the new Ag(cysteine) molecule because of the coordination of the Ag^+ ion to the nitrogen atom of the C─N bond to form a $^+NH_2Ag$ complex. Such attachment of a heavy atom like Ag (atomic mass 108) should naturally cause the C─N bond to be significantly heavy particularly on the side of the nitrogen atom and therefore distort the orientation of the molecule as would be imagined of a spring if we consider the bond to be a spring attached to two balls, one with a much heavier weight. Therefore, this end of the C─N bond should be too heavy to vibrate, and so more likely to lose the IR band due to the loss of the dipole moment.

Finally, therefore, the new Ag(Cysteine) molecule seems to contain a cysteine moiety which is present as a zwitterion (having both +ve and –ve charges). The site of the reaction between Ag NCs and cysteine is believed to be at the nitrogen atom of the cysteine molecule where it formed a Ag─N bond by coordinate bonding. Contrary to the preference of Au for the sulphur atom of the S─H bond where it forms an Au─S bond. This certainly accounts for why the S─H $_{str}$ band remained intact in both spectra in Figures 2a and b even though there may be a chance of Ag partially coordinating with sulphur (Ag^+….S─H) which could also account for the observed attenuation of this band in Figure 2b.

Electrospray Ionization Mass Spectroscopy (ESI-MS)

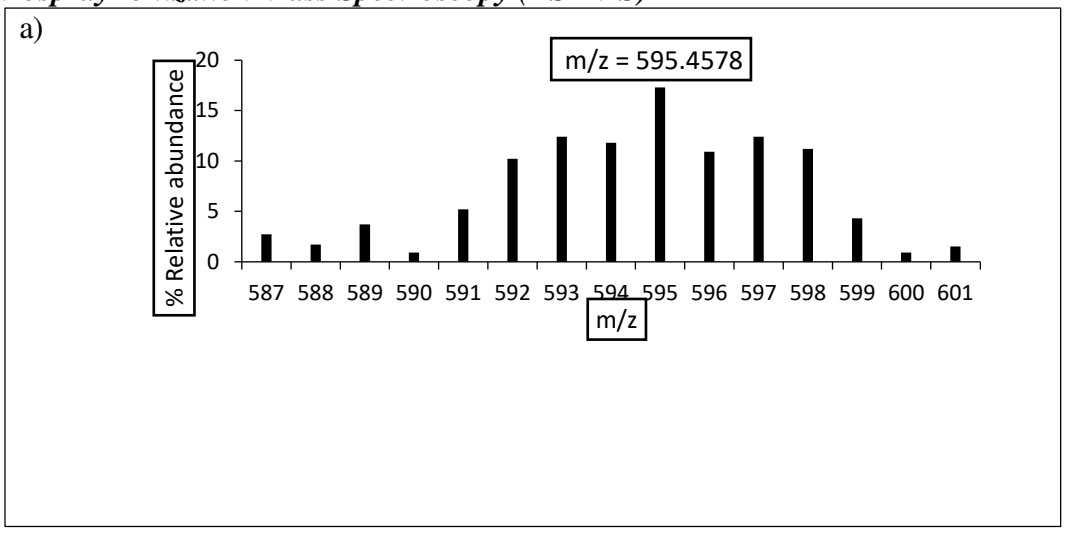

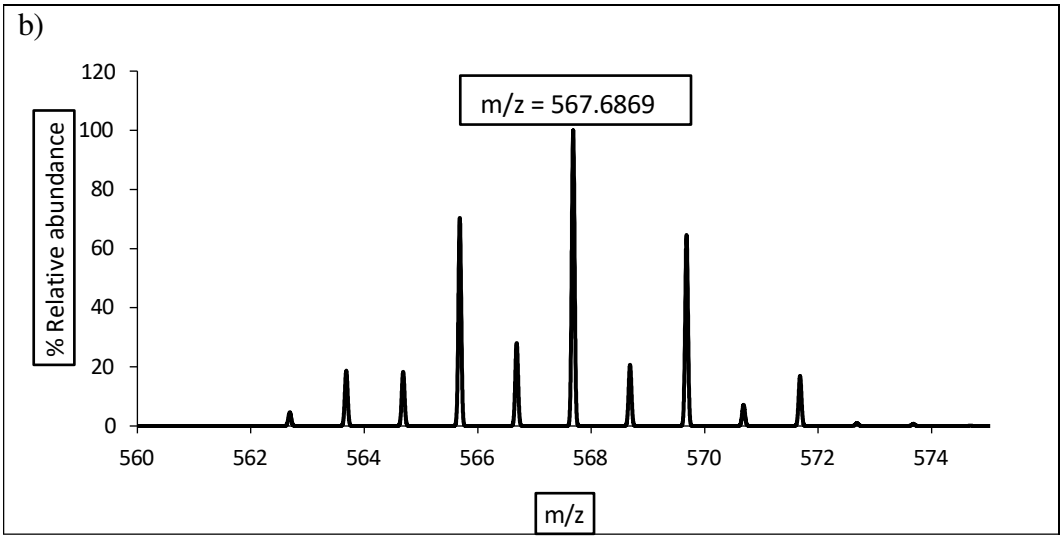

Fig. 4: ESI-MS spectrum of (**a**) Ag_4 NCs stabilized by inorganic (**$Ag_4B_3O_5.BH_3.2H_2O$-**) ligands before the exchange reaction, and (**b**) Ag_4 NCs after the exchange reaction showing the new cysteine ligands (**$Ag_4BH_4C_3H_7NO_2S$)** at **m/z = 567.6869** (experimental) ionized by loss of H^+.

The molecular formula of the as-synthesized Ag(Cysteine) molecule was confirmed using an electrospray ionization mass spectrometer (ESI-MS) instrument. This is a soft ionization technique that does not cause any significant damage to a molecule. It operates in two modes either by ionizing the sample through the loss of a proton (in the negative mode) or by the addition of a proton or ions like Na^+ (in the positive mode) and then nebulizing the sample through a vacuum where it "flies" towards the detector and is analyzed on arrival, hence it is described as time-of-flight ESI-MS.

The as-synthesized Ag(Cysteine) sample was run through the ESI-MS instrument in both the positive and negative modes with *leucine enkephalin* as the reference. The data obtained is presented in Figure 4 above. Figure 4a is the spectrum of the Ag NCs showing the full complements of passivating ligands on the Ag core. This shows that the ligand was made up of borate (B_3O_5), borane (BH_3), and two molecules of water ($2H_2O$). The split patterns on the spectrum confirm that they are consistent with Ag_4 and boron, this is according to their isotopic abundance. This in addition to incremental m/z ratios equivalent to 16, 14, 18, and another 18 completed the total mass of 595 and a molecular formula of **$Ag_4B_3O_5.BH_3.2H_2O$-**. This was considered as the control sample. In Figure 4b, the molecular formula was confirmed to be **$Ag_4BH_4C_3H_7NO_2S$-** with a molecular mass of 567.6869, showing that the sample ionized by loss of a proton H^+ with the split pattern again consistent with Ag_4 as would be expected. The apparent difference in the molecular masses of the two molecules (the borate stabilized and the new cysteine stabilized Ag_4 molecule) reflects the loss of the borate and water components of the former ligands from the initial molecule and this is taken as an important indication of successful ligand exchange reaction.

CONCLUSION

The possibility of ligand exchange between borate and borane-capped Ag NCs with cysteine biomolecule as a ligand was studied *in vitro* with the view to adopting a similar approach *in vivo*. The results showed that it should be easy to exchange the labile borate ligand with nitrogen- containing organic biomolecules like cysteine in the areas of medical and life sciences. TEM data confirmed the formation of nanoscale, seemingly spherical crystals of Ag. The FT-IR data besides confirming that the reaction was successful, also gave a lucid picture of the reaction pathway and indicated the reaction site of the Ag^+ ion on the cysteine molecule. The disappearance of both the C─O and C─N bands together with the notable difference in the size of the band at the 3200 – 3600 cm^{-1} position were also considered significant indicators of the formation of the Ag_4(Cysteine) molecule with bonding centred on the lone pair electron of the nitrogen atom at the C─N position of the amide group. It invariably inferred the preference of the Ag atom for nitrogen (atom) which resulted in the formation of an Ag─N bond via coordinate bonding, instead of an Ag─S bond as is famous with the Au and S (Au─S) bond. The ESI-MS data confirmed the molecular formula of the new product formed as Ag_4BH_4(Cysteine); that is, $Ag_4BH_4C_3H_7NO_2S$ with a molecular mass of 567.6869.

REFERENCES

An, R., Liang, Y., Deng, R., Lei, P., and Zhang, H. (2022). *Hollow nanoparticles synthesized via Ostwald ripening and their upconversion luminescence-mediated Boltzmann thermometry over a wide temperature range*. https://doi.org/10.1038/s41377-022-00867-9

Ashique, S., Garg, A. and Hussain, A. (2023). *Nanodelivery systems: An efficient and target - specific approach for drug - resistant cancers*. *August*, 18797–18825. https://doi.org/10.1002/cam4.6502

Athokpam, B., Ramesh, S. G. and McKenzie, R. H. (2017). Effect of hydrogen bonding on the infrared absorption intensity of OH stretch vibrations. *Chemical Physics*, 488–489: 43–54. https://doi.org/https://doi.org/10.1016/j.chemphys.2017.03.006

Bardhan, N. (2022). Nanomaterials in diagnostics, imaging, and delivery: Applications from COVID-19 to cancer applications? Motivation and scope. *MRS Communications*, 12(6): 1119–1139. https://doi.org/10.1557/s43579-022-00257-7

Basu, A., Tolbatov, I., Marrone, A., Vaskevich, A. and Chuntonov, L. (2024). Noble Metal Nanoparticles with Nanogel Coatings: Coinage Metal Thiolate-Stabilized Glutathione Hydrogel Shells. *The Journal of Physical Chemistry C*, 128(8): 3438–3448. https://doi.org/https://doi.org/10.1021/acs.jpcc.4c00433

Bawoke, M. and Abera, B. (2023). Nanomaterials: An overview of the synthesis, classification, characterization, and applications. *Nano Select*, 4: 486–501. https://doi.org/10.1002/nano.20230038

Campanella, A., Palleschi, V. and Legnaioli, S. (2021). Introduction to vibrational spectroscopies. *Chem. Texts*, 7(5). https://doi.org/https://doi.org/10.1007/b40828-020-00129-4

Deniz, E., Schmidt-Engler, J. M., Ulrich, K., Oberle, M., Wille, G. and Bredenbeck, J. (2022). SH—It happens S–H bonds as intrinsic 2D-IR labels in proteins. *The Journal of Chemical Physics*, 157(135102). https://doi.org/10.1063/5.0107057

Fernández-gómez, P., Pérez, C., Lastra, D., Thompson, S., Sot, B., Salas, G., Somoza, Á., Espinosa, A. and Castellanos, M. (2023). *Development in Spain: improving the treatment of diseases from the nanoscale*. *July*. https://doi.org/10.3389/fbioe.2023.1191327

Hagemann, H., Kaminski, J. W., Wesolowski, T. A., Radovan, C., Penin, N., Sørby, M. H., Hauback, B. C., Severa, G. and Jensen, C. M. (2008). LiSc (BH4) 4: A Novel Salt of Li + and Discrete Sc (BH 4) 4 - Complex Anions. *Journal of Physical Chemistry A*, 112: 7551–7555. https://doi.org/10.1021/jp803201q

Hasegawa, T. (2017). Infrared Spectroscopy as a Vibrational Spectroscopy. In *Quantitative Infrared Spectroscopy for Understanding of a Condensed Matter* (pp. 1–36). https://doi.org/https://doi.org/10.1007/978-4-431-56493-5_1

Jadhav, V., Roy, A., Kaur, K., Rai, A. K., and Rustagi, S. (2024). Recent advances in nanomaterial-based drug delivery systems. *Nano-Structures and Nano-Objects*, 37(2024). https://doi.org/https://doi.org/10.1016/j.nanoso.2024.101103.

Jebasingh, B., Sneha, A. R., Thushara, K. M., Ephrin, S. and Anna Benedict, B. (2023). Nanostructured Materials–Enabled Biosensors for Drug Delivery and Medical Diagnosis. In K. Pal (Ed.), *Nanovaccinology,* (pp. 245–257). Springer, Cham. https://doi.org/https://doi.org/10.1007/978-3-031-35395-6_14

Joudeh, N. and Linke, D. (2022). Nanoparticle classification, physicochemical properties, characterization, and applications: a comprehensive review for biologists. *Journal of Nanobiotechnology*, 20(262). https://doi.org/https://doi.org/10.1186/s12951-022-01477-8

Khalkho, B. R., Kurrey, R., Deb, M. K., Shrivas, K., Thakur, S. S., Perves, S. and Jain, V. K. (2020). L-cysteine-modified silver nanoparticles for selective and sensitive colorimetric detection of vitamin B1 in food and water samples. *Heliyon*, 6(2): e03423. https://doi.org/10.1016/j.heliyon.2020.e03423

Lan, J. (2022). *Overview of Application of Nanomaterials in Medical Domain*. *2022*.

Liu, H., Li, Y., Li, T., Mu, Y., Fang, X. and Zhang, X. (2024). Mono-, di- and trimetallic coinage nanoparticles were prepared via the Brust–Schiffrin method. *Physical Chemistry Chemical Physics*. https://doi.org/DOI

https://doi.org/10.1039/D4CP01530D

Michos, F. I., Chronis, A. G., Garoufalls, C. S. and Sigalas, M. M. (2024). Optical properties of Cu, Ag, and Au Nanoparticles with different sizes and shapes. *Applied Research*, *e202300101*. https://doi.org/10.1002/appl.202300101

Nile, S. H., Baskar, V., Selvaraj, D. and Nile, A. (2020). Nanotechnologies in Food Science: Applications, Recent Trends, and Future Perspectives. In *Nano-Micro Letters* (Vol. 12, Issue 1). Springer Singapore. https://doi.org/10.1007/s40820-020-0383-9

Oyem, H. H. (2018). *Fluorescence Silver Nanoclusters*. University of Newcastle, upon Tyne, United Kingdom.

Oyem, H. H., Houlton, A. and Horrocks, B. R. (2022). Silver nanoclusters prepared in water-in-oil emulsions. *Nano Express*, *3*(4). https://doi.org/10.1088/2632-959X/acb83a

Paunkovic, B. S., Santos, D. M. F., Lisboa, U. De and Banks, C. E. (2013). Analytical Methods. *Analytical Methods*, 5: 829–839. https://doi.org/10.1039/c2ay26077h

Phan, H. T. and Haes, A. J. (2019). What does Nanoparticle Stability Mean? *Journal Physical Chemical C Nanomaterial Interfaces*, 123(27): 16495–16507. https://doi.org/10.1021/acs.jpcc.900913

Poon, W., Kingston, B. R., Ouyang, B., Ngo, W. and Chan, W. C. W. (2020). A framework for designing delivery systems. *Nature Nanotechnology*, 15: 819–829. https://doi.org/https://doi.org/10.1038/s41565-020-0759-5

Selmani, A., Kovacevic, D. and Bohinc, K. (2022). Nanoparticles: From synthesis to applications and beyond. *Advances in Colloid and Interface Science*, 303(102640). https://doi.org/https://doi.org/10.1016/j.cis.2022.102640

Shafiq, M., Anjum, S., Hano, C., Anjum, I. and Abbasi, B. H. (2020). *An Overview of the Applications of Nanomaterials and Nanodevices in the Food Industry*. *Figure 1*, 1–27.

Smith, B. C. (2017). The C-O Bond, Part I: Introduction and the Infrared Spectroscopy of Alcohols. *Spectroscopy*, 32(1): 14–21.

Soares, S., Sousa, J., Pais, A. and Vitorino, C. (2018). *Nanomedicine: Principles, Properties, and Regulatory Issues*. 6(August), 1–15. https://doi.org/10.3389/fchem.2018.00360

Wang, Z., Dan, G., Zhang, R., Ma, L. and Ke, L. (2023). Coupling and decoupling CH stretching vibration of methylene and methine in serine conformers. *Spectrochimica Acta Part A: Molecular and Biomolecular Spectroscopy*, 285(121829). https://doi.org/https://doi.org/10.1016/j.saa.2022.121829